A Causal Concentration-Response Function for Air Pollution: Evidence from Wildfire Smoke*

Nolan H. Miller
University of Illinois
and NBER

David Molitor
University of Illinois
and NBER

Eric Zou
University of Oregon
and NBER

December 2021

Abstract

The shape of the concentration-response relationship between air pollution exposure and human health is central to determining efficient pollution regulations, especially for countries where pollution levels are already low and further abatement may be very costly. We provide the first causal estimates of the concentration-response relationship between exposure to fine particulate matter ($PM_{2.5}$) and mortality, exploiting variation from exposure to wildfire smoke. Using a novel satellite-based dataset of daily smoke plume coverage for the entire U.S. from 2007 to 2017, we find that drifting wildfire smoke is pervasive throughout the US, accounts for over 20% of average $PM_{2.5}$ concentrations, and produces air quality shocks of widely varying intensity. We link this variation to daily elderly mortality rates using administrative data on 100% of the Medicare population. We find that the concentration-response relationship between $PM_{2.5}$ and mortality caused by wildfire smoke is concave: small air pollution shocks have proportionally larger mortality effects than large air pollution shocks. Methodologically, our findings highlight nonlinear treatment effects as an important reason other than identification issues for why instrumental-variable (IV) and ordinary-least-squares (OLS) estimates of the mortality effect of pollution might differ. From a policy perspective, our results point to large benefits of additional air quality improvements in the U.S.

JEL Classification: I18, J14, Q51, Q53, Q54
Keywords: Air pollution, Mortality, Wildfire smoke, Concentration-response

*Miller: University of Illinois and NBER, nmiller@illinois.edu. Molitor: University of Illinois and NBER, dmolitor@illinois.edu. Zou: University of Oregon and NBER, ericzou@uoregon.edu. We thank Alex Hollingsworth, Edson Severnini, Nikolaos Zirogiannis, and seminar participants at McGill University, the Occasional Workshop in Environmental and Resource Economics, Princeton University, the University of Illinois, and the University of Texas at Austin for helpful comments. Research reported in this publication was supported by the National Institute on Aging of the National Institutes of Health under award numbers P01AG005842 and R01AG053350. The content is solely the responsibility of the authors and does not necessarily represent the official views of the National Institutes of Health. A previous version of the paper was circulated as "Blowing Smoke: Health Impacts of Wildfire Plume Dynamics".

1 Introduction

Decades of research have documented serious and widespread harms of air pollution on human health, leading many countries to regulate emissions and set air quality standards (Dockery et al., 1993; Schwartz, Laden and Zanobetti, 2002; Currie et al., 2014; Goldman and Dominici, 2019). Optimal policy involves reducing pollution as long as the marginal benefits of abatement exceed the marginal costs. Assessments of the optimal pollution level therefore depend greatly on the presumed shape of the concentration-response (C-R) function, which describes the marginal benefits of a reduction in air pollution concentration from a given level. Figure 1, adapted from Pope III et al. (2015), illustrates why the curvature of the C-R function matters for optimal pollution regulation: the socially optimal level of pollution is much lower if the marginal benefit of pollution abatement is considered to be a concave relationship rather than a convex one.

Prevailing academic and policy practices generally assume that the C-R relationship between pollution and health is convex, with large incremental effects at high levels of pollution and small effects at low pollution levels. Epidemiology research on the mortality effects of air pollution exposure often begins with a log-linear regression specification that implicitly assumes such a convex relationship (e.g., Krewski et al., 2009). Air quality regulations in the U.S. put exclusive focus on areas exceeding safety levels, with heavy penalties in place to prevent large pollution spikes. On the other hand, an emerging body of evidence based on cross-country comparisons suggests the C-R relationship might instead have a *concave* shape, with health damages rising sharply at initial pollution levels, and flattening out at higher levels (e.g., Pope III et al., 2011; Crouse et al., 2012; Pope III et al., 2015). A growing literature in economics uses causal approaches to identify average treatment effects of pollution exposure (Currie and Neidell, 2005; Currie, Neidell and Schmieder, 2009; Currie, 2013; Schlenker and Walker, 2016; Deryugina et al., 2019). However, these causal methods have not been applied to study the shape of the C-R relationship, in part due to the challenge of identifying quasi-experimental variation in pollution shocks of varying magnitudes.

We propose a novel quasi-experimental approach to estimate causal C-R relationships between air pollution and health, exploiting variation in ambient air pollution coming from wildfire smoke exposure. Wildfires are a major pollution source, with total emissions accounting for 20% of particulate matter pollution in the U.S. Using satellite-based measures of daily smoke plume coverage for the entire U.S. from 2007 to 2017, we find that drifting wildfire smoke generates frequent and significant variation in ground-level $PM_{2.5}$ in places far from the wildfires. We link this variation to administrative data on 100% of Medicare beneficiaries to provide the first nationwide evaluation of the mortality cost of wildfire smoke exposure among the U.S. elderly. We find that wildfire smoke exposure significantly increases mortality for the elderly. Our average treatment effect estimate suggests a 1 ug/m^3 increase in daily $PM_{2.5}$ increases elderly mortality by 0.62 deaths per million people over the next three-day period. This effect size is consistent with prior studies exploiting different quasi-experimental contexts (Deryugina et al., 2019).

The primary contribution of this paper is to improve upon the literature's estimation of average treatment effects by exploiting variation in the *magnitude* of pollution shocks due to two unique features of the smoke quasi-experiment. First, changes in fire emissions and the winds create a gradient of air quality as a function of county's distance to nearby smoke plumes. For example, compared to a "clean" day when a county is over 1,000 km away from any smoke plumes, having plumes within a 500-750 km (100-250 km) radius raises ground-level $PM_{2.5}$ by **1 ug/m^3** (**3 ug/m^3**) on average. Second, smoke plumes differ in thickness which, due to differential optical characteristics, the satellite measurements can categorize into light, medium, or thick smoke. When a county is covered by a medium-thickness smoke plume, the ground-level $PM_{2.5}$ increases on average by **7 ug/m^3**, while a thick smoke plume increases $PM_{2.5}$ by nearly **17 ug/m^3**. Based on a sample-average $PM_{2.5}$ level of 9.6 ug/m^3 during the study period, the smoke quasi-experiment allows us to examine differential mortality effects of pollution shocks ranging in magnitude from about **2% to 177%** of the mean concentration.

Our analysis produces an estimate of the causal C-R relationship: changes in the elderly mortality rate as a consequence of changes in ambient $PM_{2.5}$ of differing magnitudes. We find that this relationship is monotonically increasing but concave in shape: small air pollution shocks have proportionally larger marginal mortality damages than larger air pollution shocks. We show that this concave graphical pattern can be econometrically represented by two-stage least squares (2SLS) regressions with smoke instruments that shock $PM_{2.5}$ in different ranges: using large shocks as excluded instruments gives rise to smaller average treatment effect estimates than using small shocks. Methodologically, our finding of a non-linear C-R relationship suggests a reason why there may be so much variation among published estimates of the health effect of pollution: different estimates could arise if they exploit pollution variation at different points along the C-R curve.

The causal C-R relationship we identify is in "shock space": *changes* in the mortality rate as a function of *changes* in pollution. We benchmark these results with simple OLS estimates that give us a C-R relationship in "level space": *levels* of mortality rates at different *levels* of pollution. We find that the the 2SLS (causal) C-R relationship and OLS (correlational) C-R relationship have similar curvature. While prior discussions of differences between instrumental variables and observational estimates of pollution impacts have focused largely on identification concerns, our findings suggest instead that differential weighting of larger versus small pollution shocks can help to reconcile the differences.

Our paper raises several important policy implications. First, air quality regulation is still relevant, if not *more* important, in a low-pollution context. The concave curvature of the C-R function implies the socially optimal pollution level might be lower than previously thought, and further pollution abatement may still bring substantial health benefits. Second, because pollution exhibits nonlinear health effects, linear regression models may yield different estimates depending on the part of pollution variation being used in a particular study. Estimates using large pollution shocks are likely to produce smaller marginal effects than studies using smaller shocks. Third, the source of pollution we leverage – wildfire emissions

– is a major component of emissions with far-reaching air quality and health damages. We demonstrate that these damages are measurable with available data and econometric tools, and we note that wildfires are one of the largest source of cross-boundary externalities that are not yet subject to any environmental regulation. To facilitate future exploration, as a companion to our paper we provide processed data with the smoke shocks aggregated to various geo-temporal levels.

Section 2 continues with data description and summary statistics. Section 3 evaluates the quasi-experimental nature of the wildfire smoke shocks and presents average treatment effect estimates. Section 4 presents the concentration-response function estimation. Section 5 concludes.

2 Data

2.1 Data Description

We build a daily panel dataset of county-level wildfires smoke shocks, ambient air pollution, and elderly mortality rate. These data come from three sources.

Smoke Data. We use wildfire smoke plumes data from the National Oceanic and Atmospheric Administration's Hazard Mapping System (HMS) from 2007 to 2017. HMS incorporates imagery from nine satellites to detect wildfire smoke exposure across the United States.[1] Areas of smoke coverage ("smoke plumes") are manually outlined by smoke analysts based on visible channel imagery, with infrared occasionally employed to screen out cloud confounds. Each smoke plume constitutes up to three density contours – light, medium, and thick smoke – corresponding roughly to average densities of roughly 5, 16, and 27 micro grams of particles per cubic meter of air ($\mu g/m^3$). The contour estimation is based on the affected area's aerosol optical depth, which is a satellite measure of sunlight extinction that

[1]These satellites include the GOES-East/West, Terra, Aqua, NOAA-15/18/19, and METOP-A/B. Together, these satellites provide comprehensive spatial coverage, with over 200 looks per day in areas of overlap.

reflects the concentration of particulate pollution in the atmosphere.

Air Pollution Data. We draw ambient air pollution data from the U.S. Environmental Protection Agency's Air Quality System (AQS). The AQS contains hourly readings of several "criteria" air pollutants from in situ air monitoring stations across the country. Because the primary purpose of the AQS is to detect violation of national clean air standards, the monitoring network tend to mostly cover urban areas. To maximize spatial coverage, we adopt inverse distance weighting, a common spatial interpolation technique used in atmospheric science and environmental economics, where a county's pollution concentration is calculated as the inverse-distance-weighted average of readings from all monitoring sites within 20 miles of the county's geographic centroid. About 27% county-days in the sample have available $PM_{2.5}$ values.

Mortality Data. Our county-by-daily level mortality variable is constructed from the Medicare's Master Beneficiary Summary File (MBSF). MBSF is an annual directory of all beneficiaries enrolled in the Medicare program. We observe each beneficiary's residential county and, for decedents who died that year, the date of death. There are two advantages of measuring elderly mortality rate using the MBSF. First, Medicare is a mandatory government insurance program for the elderly in the U.S. Over our study period, the MBSF covers over 97% of the US population aged 65 and older, giving us a comprehensive measure of elderly mortality. Second, Medicare's date of death field is cross-verified with records kept by the Social Security Administration. This feature allows us to measure mortality rate accurately at the *daily* level, which is critical for our research design that leverages high-frequency pollution shocks.

2.2 Defining "Smoke Shocks"

Figure 2 shows a day-snapshot of the smoke shapefiles on August 22, 2013. The large, light-colored contour represents smoke plumes observed across the CONUS on that day. The largest plume can be seen originating from the Rim Fire of the state of California. The

medium- and dark-colored contours represent locations of thicker smoke plumes.

This snapshot exemplifies two general features of wildfire smoke exposure. First, smoke plumes are far reaching. Smoke emitted from a fire event in the western United States can well reach the midwest in several days. Massive movements of smoke plumes create abundant spatial and temporal variation in counties' exposure. Second, fires frequently emit dense smoke plumes. Such intensive exposure events do not only occur in the immediate vicinity of the fire itself. Figure 2 shows big swaths of Oregon and Nevada are covered by medium and thick smoke plumes from the Rim Fire.

The key independent variables of our paper is a series of indicators for "smoke shocks", defined as a function of a county's distance to the nearest wildfire smoke plume and, if the county is covered by a smoke plume, the density of the plume. Consider one of the smoke shock variables we call the "0-100 km" shock. This is an indicator variable that equals 1 if the county-day is within 100 km to the nearest smoke plume.[2] Similar indicators are defined for five other distance bins: 100-250 km, 250-500 km, $\cdots$, >1000 km. We have three additional indicators for if the county is covered by light, medium, and thick smoke plumes. In total, this gives us nine smoke shock indicators. Note that any county-day in our data will fall into one of these nine categories. In regression analysis, we will use ">1000 km" as the reference group, and estimate how smoke changes air pollution and mortality rate relative to these "clean" days.

Figure 3 summarizes the frequency distribution of different smoke shocks. Note the three bars to the right of the vertical dashed line show that U.S. counties are covered by smoke plumes 10.5% of the days during out study period. This means the average county is covered by wildfire smoke plumes by about 38 days per year. Figure 4 maps out the geographic distribution of smoke coverage. A distinct pattern is that smoke coverage is the most common in the midwest states such as Minnesota, North Dakota, and Iowa. Although these states do

[2]In practice, we develop a geo-computation routine that flags the county as "within 100 km" to a plume if at least 20% of the county's land area is covered by a 100-km buffer polygon around the original smoke plume shapefile.

not have many wildfire incidents, they experience downwind emissions from wildfires in the west and from Canada. Several southern states such as Louisiana and Florida experience frequent smoke shocks from both local fire events and transported wildfire pollution from Mexico and the South Americas.

Our final sample is a balanced daily panel of counties in the contiguous US from 2007 to 2017, with a total of about 13 million observations. About 73% of county-days are missing $PM_{2.5}$ observations due to sparsity of the monitoring network. In our analysis below, we estimate the "reduced form" mortality-smoke relationship using the full sample. Instrumental variable estimation uses the restricted sample where $PM_{2.5}$ observations are available.

3 Wildfire Smoke, Air Pollution, and Elderly Mortality

We begin with event study evidence in this section, with the aim of verifying that drifting smoke plumes can provide exogenous shocks to local air quality and elderly mortality. We collapse smoke shocks of various magnitudes (Section 2.2) into a single smoke event index, and estimate how air pollution and elderly mortality rate respond to these smoke events.

3.1 Estimation Equation

Our goal is to model and estimate how ground-level air pollution and mortality rate change as a function of time since smoke hits an area. Using observations for each county c and date t, we estimate the following event study specification:

$$\begin{aligned} Y_{ct} = & \sum_{d=-20}^{20} \beta_d \, SmokeIndex_{c(t-d)} \\ & + \left[\text{county} \times \text{day-of-year FEs}\right]_{ct} + \left[\text{state} \times \text{year} \times \text{month FEs}\right]_{ct} + \varepsilon_{ct}. \end{aligned} \tag{1}$$

The key independent variable is $SmokeIndex_{ct}$, defined as a sum of scaled smoke shocks in county c on date t. The scalars are chosen to approximate the same-day effect of each type of

shock on ground-level $PM_{2.5}$. By construction, a 1-unit increase in the index will correspond to an increase of approximately 1 $\mu g/m^3$ in ground-level $PM_{2.5}$ on the day of the event. This scaling facilitates interpreting the effects of a smoke index event over time and across outcomes.

The key event study parameters of interest in equation (1) are the β_d's, each representing the effect of smoke observed on date $t-d$ on date t's outcome. The β_d's therefore represent changes in the outcome variable from 20 days before to 20 days after the smoke-event day. Outcomes Y_{ct} are ground-level $PM_{2.5}$ ($\mu g/m^3$) and mortality (deaths per million). Observations are weighted by the Medicare population in county c on date t, and standard errors are clustered at both the county and date levels.

The regression equation includes two main sets of fixed effects. The county-by-day-of-year fixed effects control flexibly for county-specific seasonal correlations between smoke, pollution, and mortality. These fixed effects essentially ensure that we compare the same county on the same day of the year, but across years with different smoke exposure. The state-by-year-by-month fixed effects control for state-specific time-varying shocks such as changes in local environmental or health policies. Our identifying assumption is that, conditional on the fixed effects, the remaining variation in *SmokeIndex* is as good as random. The event study specification allows us to assess the validity of the identifying assumption by inspecting a zero (flat) pre-trend of estimated $\hat{\beta}$'s.

Errors in Smoke Measurement. The boundary of the smoke plume shapefiles represent analysts' judgement about where the bulk of the wildfire smoke is, and it need not always correspond to the true extent of pollution increases. As we show below, counties outside of smoke plumes may still experience mild rises in ground-level $PM_{2.5}$. By measuring shocks based on flexible distance-to-smoke bins rather than simple covered-by-shapefiles-or-not status, our approach explores much richer variation and makes the analysis less prone to measurement errors in the smoke data.

One major robustness check we do is to replace the analyst-based HMS smoke measure

with similar data generated by NOAA's HYSPLIT model, an entirely machine-based smoke nowcasting and forecasting algorithm.[3] It bears mentioning that, although the automated smoke analysis is not subject to human biases, it is prone to modeling errors. In fact, consistency between HYSPLIT's nowcasts and HMS smoke files is an important verification metric NOAA uses to assess reliability of HYSPLIT's smoke forecasts. In unreported analysis, we find that using HYSPLIT smoke measure gives rise to very similar results.

Smoke versus Other Transported Pollution. The primary driver of smoke plumes movements is the wind. Winds can transport air pollutants other than those generated by the wildfire, such as those from industrial sources. This raises the question whether our pollution and mortality estimates capture the pure effects of wildfire smoke.

We note that, from a purely instrumental variable perspective, it does not matter whether winds carry non-wildfire pollution to the county: all it requires is that winds generate significant changes in local air pollution and would not influence mortality rates otherwise. However, our concentration-response analysis does rely on the assumption that it is wildfire smoke, rather than pollution from other sources, that leads to changes in local air quality, for otherwise there is no reason to think thicker smoke plumes would generate larger pollution shocks.

We address this concern by estimating an augmented version of equation (1) that includes a set of 60-arc-degree bins of local daily wind directions, each interacted with county indicators, à la Deryugina et al. (2019). These wind direction covariates capture transported pollution from fixed point sources, e.g., an industrial cluster to the north of a county that increases a county's pollution *whenever* winds are blowing from the north. We have confirmed that controlling for these local wind direction variation has a limited impact on the event study estimation of pollution responses. This evidence suggests that the HMS does a good job discerning wildfire pollution from other pollution sources.

[3]The smoke HYSPLIT, or the Hybrid Single Particle Lagrangian Integrated Trajectory model, is developed by NOAA's Air Rsources Laboratory to provide daily forecast of smoke emissions and dispersion. The smoke shapefiles we use are from HYSPLIT smoke *analysis* file, which uses day $t-1$'s fire emissions and meteorology data to "nowcast" smoke conditions for day t.

Wildfire Pollution versus Industrial Pollution. A deeper concern is that biomass burning may produce a different mix of pollutants – including a higher share of volatile organic compounds (VOCs) – than emissions from car exhaust and industrial activities. To what extent does the health effect estimates derived from the wildfire quasi-experiment reflect the effect of exposure to "typical" $PM_{2.5}$ pollution? We will describe later that, when averaging across effects from large and small pollution shocks, our estimated mortality effect size on a per-unit-increase-in-$PM_{2.5}$ term is consistent with prior quasi-experimental studies that examine pollution from non-wildfire sources. Thus, the wildfire quasi-experiment replicates the existing average treatment effect estimates of $PM_{2.5}$ exposure, while allowing us to examine the underlying concentration-response relationship.

3.2 Results

Figure 5a summarizes the event study coefficients $\hat{\beta}_d$'s from equation (1) when ground-level $PM_{2.5}$ concentration is the outcome variable. $PM_{2.5}$ increased mildly on the day before the smoke shock, peaked on the smoke day (day 0 of the horizontal axis), and quickly returned to the level prior to the smoke shock. Note the magnitude of the smoke day $PM_{2.5}$ increase is 1 ug/m^3 by construction of the *SmokeIndex* variable (Section 3.1). The "jump" in pollution around day 0 suggests that ground-level changes in air pollution lines up well with the timing when smoke is detected by the satellite in the same area. This increases our confidence in the accuracy of the smoke measure. Figure 5a also shows that, except for the jump, pollution pattern is otherwise flat and stable within the 41-day time window, supporting the zero pre-trend assumption that pollution would have followed a stable path in the absence of the smoke shock.

We now repeat the same analysis but use Medicare mortality rate as the outcome variable. Figure 5b echoes the pattern in Figure 5a, with a significant increase in mortality rate in the three days following a smoke shock. The magnitude of the increase is 0.2 deaths per million Medicare beneficiaries on the smoke day, and a total increase of 0.6 deaths per

million beneficiaries over the next 3-day period. The zero pre-trend assumption also hold in the mortality context, with most of the $\hat{\beta}_d$'s coefficients move around zero except for the significant jump following the smoke day.

Two other data patterns bear highlighting. First, the initial increase in mortality around the smoke day is not compensated by subsequent mortality *reductions* within the 20-day post window we examine. This suggests that smoke's damage on mortality does not occur through "displacement," where the smoke shock would expedite deaths of already-sick individuals by a short period of time, therefore having limited welfare implications from a medium- or long-run perspective. Second, smoke shocks raise both pollution and mortality for some three days. To capture such dynamic effects, in all subsequent analysis we define pollution and mortality variables over a three-day time window. Hence, we would examine how a smoke shock on day t changes the average pollution level across days t, $t+1$, and $t+2$, as well as the total mortality within that three-day window.

The key takeaway from the event study figures is that wildfire smoke events provide "clean" shocks to ground-level air quality, with prompt impacts on elderly mortality. We are now ready to decompose $SmokeIndex$ variable at examine heterogeneous mortality impacts of large versus small pollution shocks.

4 Concentration-Response Estimates

The event study results demonstrate that acute wildfire smoke events increase ambient air pollution concentrations and mortality, with effects lingering for a few days after the event. In this section, we examine how these effects scale with the intensity of the smoke event. We first estimate how ground-level air pollution and elderly mortality respond to wildfire smoke shocks of different magnitudes. Combining the pollution and mortality estimates allows for a graphical representation of the concentration-response function (Section 4.1). We then estimate the concentration-response function curvature using an instrumental variable

approach (Section 4.2) by using smaller versus larger smoke shocks.

4.1 How Pollution and Mortality Scale with Smoke Intensity

We estimate the relationship between air pollution from wildfire smoke and health, allowing for the possibility that the relationship may be nonlinear in the size of the pollution shock. For example, "threshold" models of pollution damages predict that air pollution reductions below some level offer no benefits. Conversely, the health effects of incremental changes in pollution could be greatest at low levels of exposure.

Using observations for each county c and date t, we estimate the following specification to capture arbitrary nonlinearity in the effects of larger versus smaller smoke shocks:

$$\begin{aligned} Y_{ct} = &\sum_{s \in S} \beta_s^Y \mathbf{1}(SmokeShock_{ct} = s) \; + \; [\text{2 leads/lags of } SmokeShocks]_{ct} \\ &+ [\text{county} \times \text{day-of-year}]_{ct} \; + \; [\text{state} \times \text{year} \times \text{month}]_{ct} \; + \; \varepsilon_{ct} \end{aligned} \tag{2}$$

Outcomes Y_{ct} are 3-day measures of either ground-level $PM_{2.5}$ ($\mu g/m^3$) or mortality (deaths per million). The fixed effects are the same as equation (1). The focal independent variables are the indicators $\mathbf{1}(SmokeShock_{ct} = s)$, which measure whether county c was exposed to a smoke shock of intensity s as listed in Figure 3. We control for two leads and two lags of these smoke shocks, to isolate the impact of the shock on date t. The omitted smoke shock category is being greater than 1,000 km from a smoke plume. Thus, the coefficients β_s^Y describe the effect on outcome Y of being exposed to a smoke shock of intensity s, relative to having been at least 1,000 km in distance from a smoke plume. Observations are weighted by the Medicare population in county c on date t, and standard errors are clustered at both the county and date levels.

4.1.1 "Dose" effects of smoke shocks on ground-level $PM_{2.5}$

We first estimate equation (2) using pollution monitor readings as the outcome to yield the "dose" impact of each smoke shock on ground-level air quality. Figure 6a plots these results: 3-day ground-level $PM_{2.5}$ rises with smoke plume proximity, with the largest increases for dense plume coverage. These results also demonstrate the usefulness of smoke exposure for studying a range of pollution shocks, from increasing $PM_{2.5}$ by 0.2 $\mu g/m^3$ to over 16 $\mu g/m^3$ (over twice the mean on a reference day).

The $PM_{2.5}$ effects reported in figure 6a can be combined with the frequency of each type of smoke shock to calculate the contribution of wildfire smoke to ambient $PM_{2.5}$ over the sample period. Specifically, we calculate

$$\sum_{s \in S} \hat{\beta}_s^{\mathrm{PM}_{2.5}} Pr(SmokeShock_{ct} = s),$$

where $\hat{\beta}_s^{\mathrm{PM}_{2.5}}$ is the estimated $PM_{2.5}$ effect from smoke shock s, and $Pr(SmokeShock_{ct} = s)$ is the average fraction of days on which this type of smoke shock occurs, as reported in Figure 3. This sum equals 2.2 $\mu g/m^3$ (95% CI, 1.8–2.7 $\mu g/m^3$). Compared to the average daily $PM_{2.5}$ of 9.6 $\mu g/m^3$, these results imply that smoke accounts for 23% of ambient daily $PM_{2.5}$ in the U.S. in our sample. These findings complement EPA National Emissions Inventory estimates that wildfires produced 18% of $PM_{2.5}$ emissions in 2007–2017.[4]

4.1.2 Mortality response to smoke shocks

Next, we estimate equation (2) using 3-day mortality as the outcome. Figure 6b plots these results: 3-day mortality rises with smoke plume proximity and the density of smoke plume coverage. As we did with the pollution effects, we combine the mortality effects of each smoke plume shock with the frequency of each shock to calculate that the average daily effect of smoke on mortality is 0.98 elderly deaths per million, or 358 deaths per million per year.

[4]See https://www.epa.gov/air-emissions-inventories/air-pollutant-emissions-trends-data

Compared to an average annual mortality rate of 44,200 per million elderly, wildfire smoke accounts for 1 out of every 125 (0.8%) elderly deaths. Scaled by the Medicare population of 48 million in 2017, this corresponds to 17,300 premature elderly deaths per year.

A standard way to assess the annual mortality cost of wildfire smoke is to multiply the number of excess deaths by a value of a statistical life (VSL). The EPA recommends using a VSL of $9.8 million ($2021), which yields an estimated mortality cost of wildfire smoke of about $170 billion per year. A potential weakness of the EPA approach is that it does not adjust for the fact that decedents may have shorter than average remaining life expectancy. As an alternative approach, we assume that those dying prematurely from wildfire smoke would have lived an additional 3.5 years, based on the estimated life years lost from those dying of acute $PM_{2.5}$ exposure (Deryugina et al. (2019)). Using a value of $100,000 per life year lost yields an estimated mortality cost of wildfire smoke of just over $6 billion annually.

By comparison, wildfires account for $617 million in annual damages to structures and cost an additional $3.5 billion in federal and state suppression and protection efforts (National Institute of Standards and Technology, 2017). While these losses and costs are large, they are smaller than the estimated $6–$170 billion in the annual mortality cost of the drifting smoke.

4.1.3 Dose-response relationship between mortality and $PM_{2.5}$

We now combine the $PM_{2.5}$ "dose" effect of each wildfire smoke shock with its corresponding mortality effect to trace out a dose-response relationship between mortality and $PM_{2.5}$. The results are shown in Figure 7. Each point on this curve corresponds to one of the 9 smoke shocks included in equation 2. The horizontal position of the point for smoke shock s is given by the "dose" effect $\hat{\beta}_s^{PM_{2.5}}$ of the shock, while the vertical position is given by the mortality effect.

We note three important characteristics of the dose-response relationship shown in Figure 7. First, it is increasing and monotonic, meaning that larger pollution shocks lead

to larger mortality increases. Second, the curve is concave, implying that large air pollution shocks have proportionally smaller mortality effects than smaller air pollution shocks. Third—and an implication of this concavity—is that small pollution shocks are detrimental to health, suggesting that incremental improvements in air quality are large. In fact, these findings suggest that the benefits from additional air quality improvements may grow as the air becomes cleaner.

4.2 Instrumental Variable Estimation

In the previous section, we estimated the first-stage "dose" effects of smoke shocks of varying intensity, along with the reduced form effects of these same shocks on mortality outcomes. The slope of the resulting dose-response curve (Figure 7) can be interpreted as an instrumental variables estimate of the effect of $PM_{2.5}$ on mortality. We can directly estimate the slope over a given portion of the curve using two-stage least squares (2SLS) regression by using smoke shocks as instruments, and only excluding the smoke instruments that lead to $PM_{2.5}$ effects in the desired range. Specifically, we estimate

$$\begin{aligned}[\text{3-day mortality}]_{ct} = \beta^{IV} &[\text{3-day } PM_{2.5}]_{ct} \\ &+ [\mathit{SmokeShocks} \notin S_{\mathit{excluded}}]_{ct} + [\text{2 leads/lags of } \mathit{SmokeShocks}]_{ct} \\ &+ [\text{county} \times \text{day-of-year}]_{ct} + [\text{state} \times \text{year} \times \text{month}]_{ct} + \varepsilon_{ct}\end{aligned} \tag{3}$$

via 2SLS, instrumenting for 3-day $PM_{2.5}$ using a selection of smoke shocks in S_{excluded}. We estimate equation (3) using three different sets of excluded instruments: "large" shocks (light, medium, or thick smoke coverage), "small" shocks (not covered by smoke, but within 1,000 km of a plume), and all shocks. Observations are weighted by the Medicare population in county c on date t, and standard errors are clustered at both the county and date levels.

The results of estimating equation (3) are shown in Table 1. Column (1) reports that, for large pollution shocks, one additional unit ($\mu g/m^3$) of 3-day $PM_{2.5}$ corresponds to an

additional 0.18 deaths per million over a 3-day window. This value aligns with average slope of the upper end of the dose-response curve in Figure 7. Column (2) reports that, for smaller pollution shocks, each additional unit of $PM_{2.5}$ corresponds to an additional 0.64 deaths per million. Column (3) reports that when averaging across both large and small pollution shocks by using all smoke shocks as instruments, each unit of $PM_{2.5}$ corresponds to an additional 0.37 deaths per million, on average.

We note three things about IV estimates. First, the differences in the estimated effect of an additional unit of $PM_{2.5}$ varies substantially based on whether it comes from smaller versus larger pollution shocks. The effect of an additional unit of pollution from a small shock is over 3.5 times as large as that of an additional unit of pollution from a large shock. Moreover, these differences are statistically significant: the 95% confidence intervals of estimates in columns (1)–(3) of Table 1 are non-overlapping.

Second, we consider how the effects of pollution from wildfire smoke compare to prior estimates of the effects of $PM_{2.5}$ pollution. To do so, we compare our IV estimates to those from Deryugina et al. (2019), who use daily variation in wind direction to estimate the effects of $PM_{2.5}$. Because Deryugina et al. (2019) relate 3-day mortality to 1-day $PM_{2.5}$, we estimate a version of equation (3) using 1-day $PM_{2.5}$ in lieu of 3-day $PM_{2.5}$ to make the interpretation of our estimates comparable. We report the results in Table 2. Columns (1)–(3) show that relating our mortality effects to 1-day $PM_{2.5}$ results in estimates that are about twice as large as when relating them to 3-day $PM_{2.5}$. This is as expected, since about half of the 3-day $PM_{2.5}$ effect occurs on the first day. Column (4) reports the wind IV results from Table 2 of Deryugina et al. (2019). That estimate is nearly identical to the estimate in column (3), based on using all smoke shocks, suggesting that the mortality effects of smoke are similar on average to the mortality effects of $PM_{2.5}$ from other sources.

A third thing we note about the IV estimates using smoke shocks is how they compare to an observational estimate of the relationship between $PM_{2.5}$ and 3-day mortality. We estimate equation (3) via OLS, modified to exclude the $SmokeShocks_{ct}$ controls and instead

controlling for 2 leads and lags of observed $PM_{2.5}$. The results are reported in column (4) of Table 1: each additional unit of $PM_{2.5}$ corresponds to an additional 0.16 deaths per million over 3 days. Interestingly, the OLS result is very similar to the IV result based on large pollution shocks. Because OLS can be thought of a weighted average, with larger weights where there is more variation in treatment exposure, these findings indicate that one reason OLS estimates of pollution exposure may be smaller than IV estimates is because they place more weight on large pollution shocks.

As a final exploration of IV versus OLS estimates, we estimate an observational version of the concentration-response curve. To do so, we estimate the same observational equation as before (used to generate the result in column (4) of Table 1), but we replace the continuous measure of $PM_{2.5}$ with bins. The results, reported in Figure 8, reveal a concentration-response function that has very similar curvature to the response function estimated using variation in pollution from smoke shocks.

5 Conclusion

Our analysis estimates, for the first time, a causal concentration-response relationship between air pollution and health using quasi-experimental exposures to wildfire smoke shocks of varying size. Our analysis employs a 100% sample of elderly Medicare beneficiaries, making it geographically and demographically representative of the US elderly. We find strong evidence that the concentration-response relationship is concave, with the marginal impact of large shocks being smaller than the marginal impact of small ones. The implied shape of the concentration-response relationship is similar whether it is estimated using our preferred IV specification or an OLS approach.

The concave relationship between pollution exposure and health that our analysis highlights is important for air pollution policy, which tends to focus on the largest pollution events and the most polluted areas. Furthermore, air quality regulations in the United States fre-

quently assume a threshold level of exposure below which there are no adverse health effects (McGartland et al., 2017; Castle and Revesz, 2018; National Research Council, 2009). Concavity of the concentration-response relationship calls into question the justification for these views. Our analysis indicates that smaller shocks in less polluted areas should not be ignored. The marginal benefit of preventing such exposure events may, in fact, be larger than that of policies aimed at larger shocks. To the extent that these small shocks may be more frequent than larger ones, this makes the consideration of smaller exposure/cleaner areas even more important. In addition, our approach enables us to directly address the question of whether a threshold level of exposure exists, and our finding of the largest marginal harm at the smallest levels of pollution suggests that the existence of a safe threshold for air pollution exposure should be rejected.

Our analysis also has implications for the question of whether wealthy countries such as the Unites States, which already have relatively clean air, should continue to work toward reducing air pollution even further, or whether funds invested in reducing pollution could be redirected to other uses where they would have a larger impact on health. The fact that smaller shocks and/or exposures in cleaner places have a larger marginal impact on health suggest that continuing to devote resources to pollution abatement in these places may be justified. In fact, the aggregate benefits to moving an area from "very clean" to "extremely clean" may be larger than a similar-sized reduction in average pollution levels in more polluted areas. From a global perspective, our results have important implications for thinking about environmental justice, since they suggest that poorer countries with more polluted air may have smaller marginal benefits from pollution reduction despite having larger potential benefits *in the aggregate* from reducing pollution to the levels found in richer nations (Organization et al., 2016).

References

Castle, Kimberly M, and Richard L Revesz. 2018. "Environmental standards, thresholds, and the next battleground of climate change regulations." *Minn. L. Rev.*, 103: 1349.

Crouse, Dan L, Paul A Peters, Aaron van Donkelaar, Mark S Goldberg, Paul J Villeneuve, Orly Brion, Saeeda Khan, Dominic Odwa Atari, Michael Jerrett, C Arden Pope III, et al. 2012. "Risk of nonaccidental and cardiovascular mortality in relation to long-term exposure to low concentrations of fine particulate matter: a Canadian national-level cohort study." *Environmental health perspectives*, 120(5): 708–714.

Currie, Janet. 2013. "Pollution and infant health." *Child development perspectives*, 7(4): 237–242.

Currie, Janet, and Matthew Neidell. 2005. "Air pollution and infant health: what can we learn from California's recent experience?" *The Quarterly Journal of Economics*, 120(3): 1003–1030.

Currie, Janet, Joshua Graff Zivin, Jamie Mullins, and Matthew Neidell. 2014. "What do we know about short-and long-term effects of early-life exposure to pollution?" *Annu. Rev. Resour. Econ.*, 6(1): 217–247.

Currie, Janet, Matthew Neidell, and Johannes F Schmieder. 2009. "Air pollution and infant health: Lessons from New Jersey." *Journal of health economics*, 28(3): 688–703.

Deryugina, Tatyana, Garth Heutel, Nolan H Miller, David Molitor, and Julian Reif. 2019. "The mortality and medical costs of air pollution: Evidence from changes in wind direction." *American Economic Review*, 109(12): 4178–4219.

Dockery, Douglas W, C Arden Pope, Xiping Xu, John D Spengler, James H Ware, Martha E Fay, Benjamin G Ferris Jr, and Frank E Speizer. 1993. "An association between air pollution and mortality in six US cities." *New England journal of medicine*, 329(24): 1753–1759.

Goldman, Gretchen T, and Francesca Dominici. 2019. "Don't abandon evidence and process on air pollution policy." *Science*, 363(6434): 1398–1400.

Krewski, Daniel, Michael Jerrett, Richard T Burnett, Renjun Ma, Edward Hughes, Yuanli Shi, Michelle C Turner, C Arden Pope III, George Thurston, Eugenia E Calle, et al. 2009. *Extended follow-up and spatial analysis of the American Cancer Society study linking particulate air pollution and mortality.* Health Effects Institute Boston, MA.

McGartland, Al, Richard Revesz, Daniel A Axelrad, Chris Dockins, Patrice Sutton, and Tracey J Woodruff. 2017. "Estimating the health benefits of environmental regulations." *Science*, 357(6350): 457–458.

National Research Council. 2009. *Science and Decisions: Advancing Risk Assessment.* Washington, DC:The National Academies Press.

Organization, World Health, et al. 2016. "Ambient air pollution: A global assessment of exposure and burden of disease."

Pope III, C Arden, Maureen Cropper, Jay Coggins, and Aaron Cohen. 2015. "Health benefits of air pollution abatement policy: Role of the shape of the concentration–response function." *Journal of the Air & Waste Management Association*, 65(5): 516–522.

Pope III, C Arden, Richard T Burnett, Michelle C Turner, Aaron Cohen, Daniel Krewski, Michael Jerrett, Susan M Gapstur, and Michael J Thun. 2011. "Lung cancer and cardiovascular disease mortality associated with ambient air pollution and cigarette smoke: shape of the exposure–response relationships." *Environmental health per-*

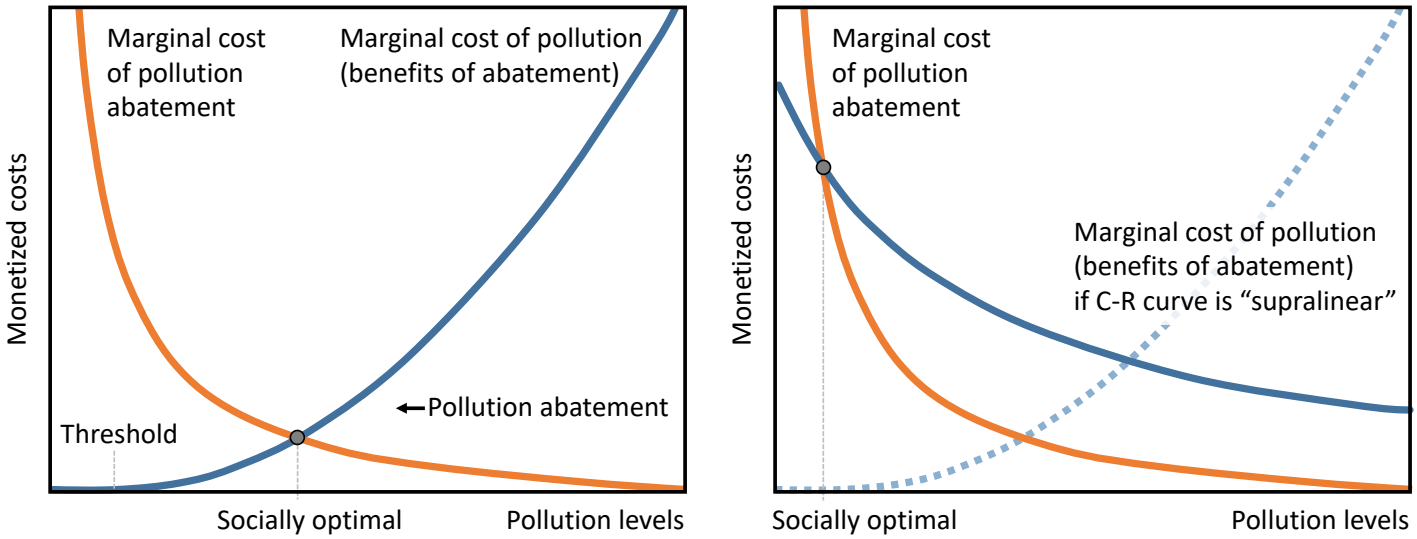
spectives, 119(11): 1616–1621.

Schlenker, Wolfram, and W Reed Walker. 2016. "Airports, air pollution, and contemporaneous health." *The Review of Economic Studies*, 83(2): 768–809.

Schwartz, Joel, Francine Laden, and Antonella Zanobetti. 2002. "The concentration-response relation between PM (2.5) and daily deaths." *Environmental health perspectives*, 110(10): 1025–1029.

Figures

Figure 1: Role of the concentration-response function for optimal pollution abatement

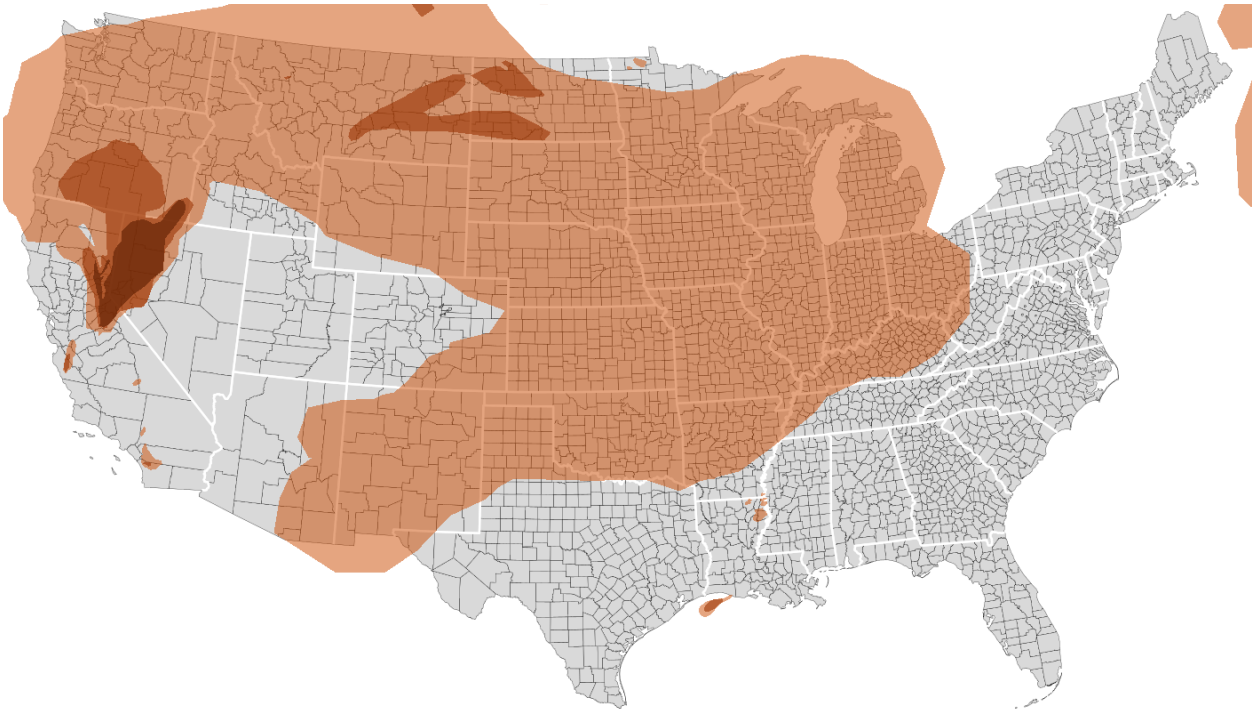


(a) Increasing marginal cost of pollution

(b) Decreasing marginal cost of pollution

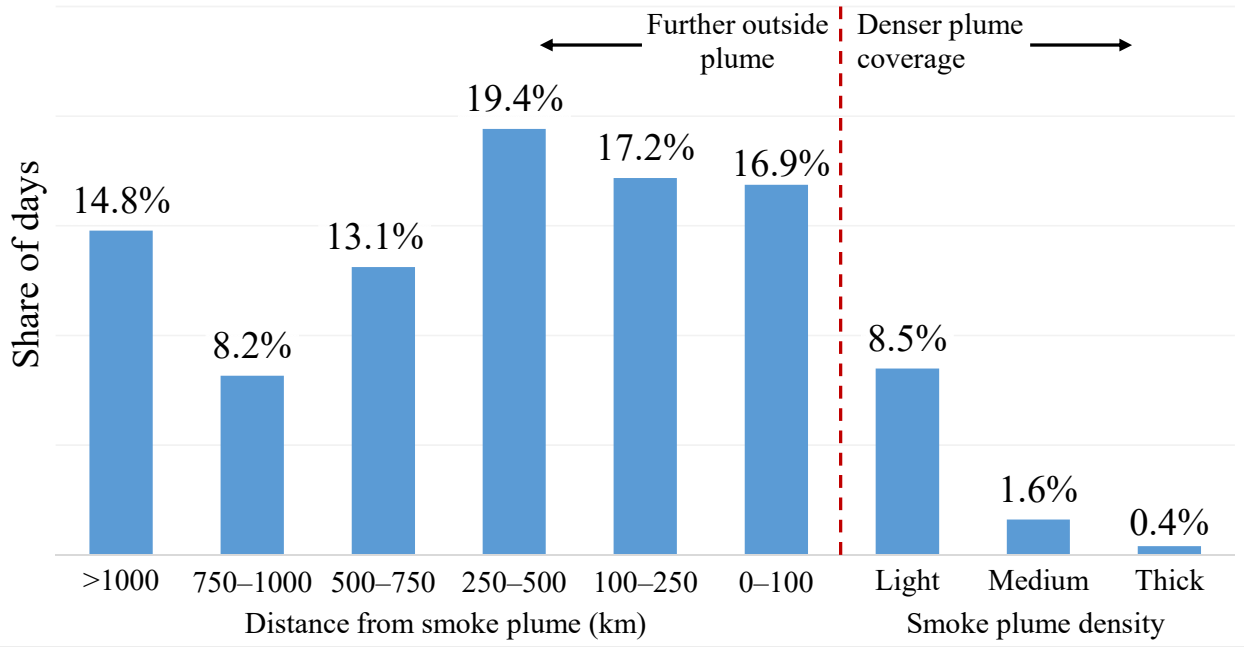
Notes: Traditional conceptual framework for economic analysis of marginal cost versus marginal benefits of pollution abatement. Adapted from Figure 1 of Pope III et al. (2015).

Figure 2: Satellite-Based Smoke Plumes (NOAA Hazard Mapping System)



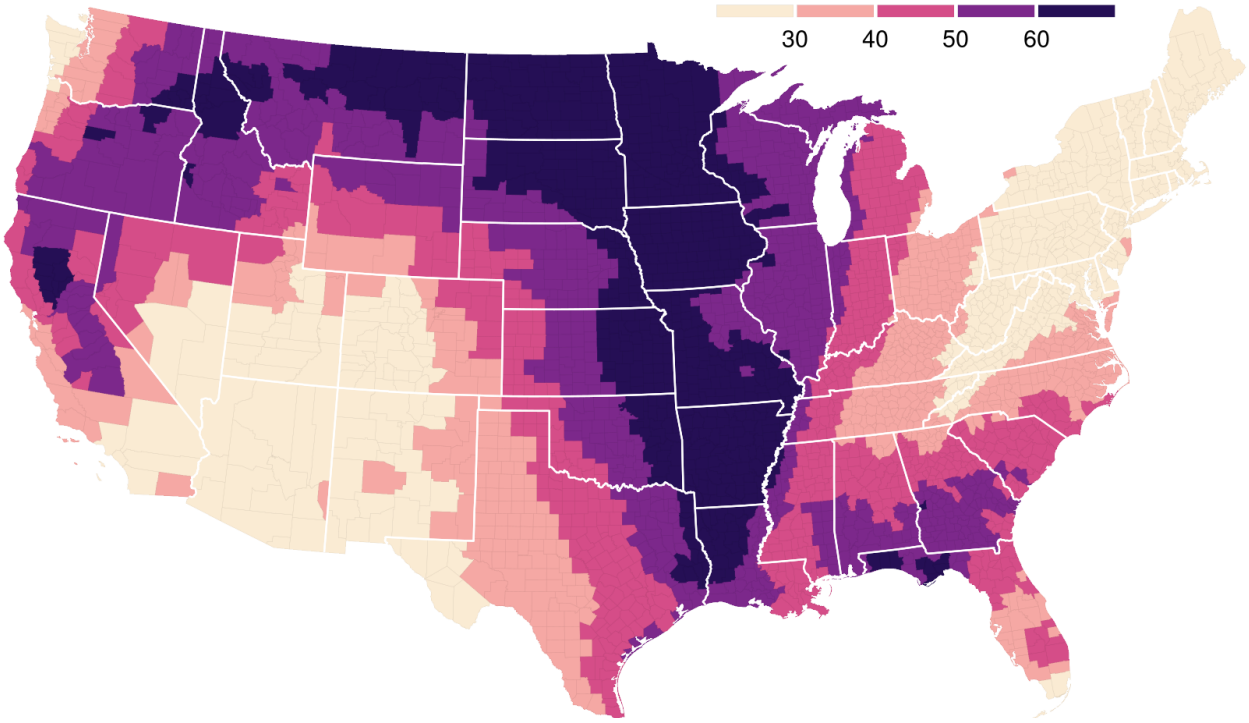
Notes: The figure shows satellite-based wildfire smoke plume contours of light, medium, and thick smoke as captured by the NOAA Hazard Mapping System on August 22, 2013. Much of this smoke is linked to the Rim Fire, which started on August 17, 2013, and stands as the 10th largest widfire on record in California.

Figure 3: Distribution of smoke shocks



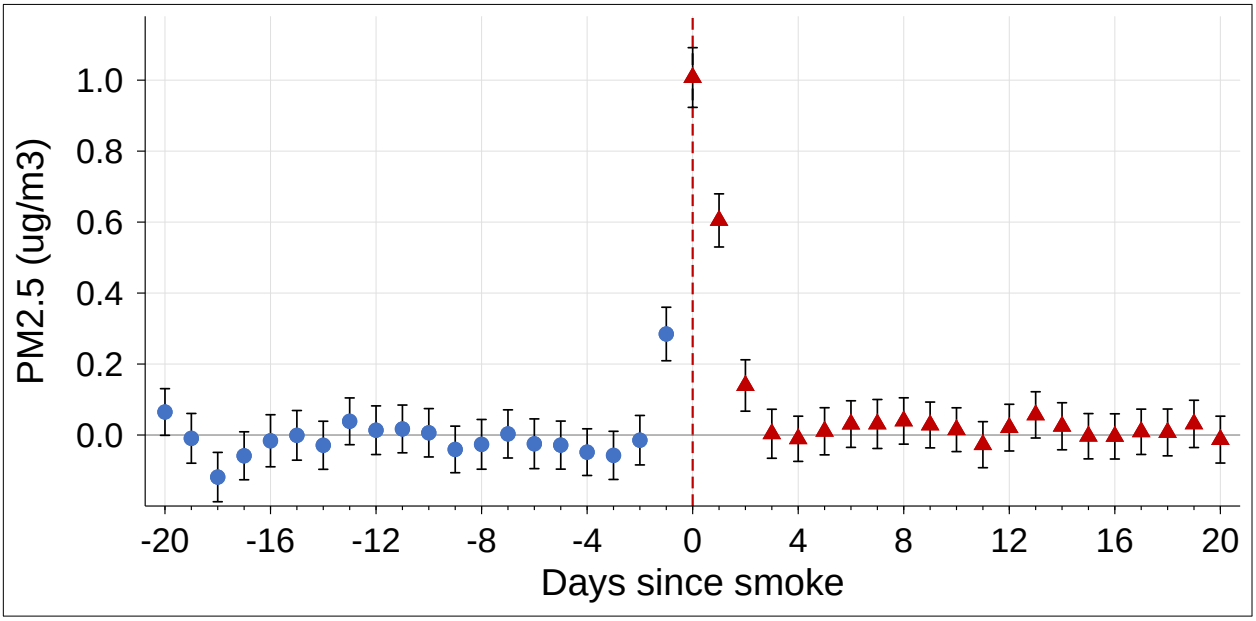
Notes: The figure shows the distribution of exposure to various smoke shocks among daily county observations in the sample. The distribution is weighted by county Medicare population. The smoke shock categories listed here are mutually exclusive.

Figure 4: Number of days per year with smoke plume coverage

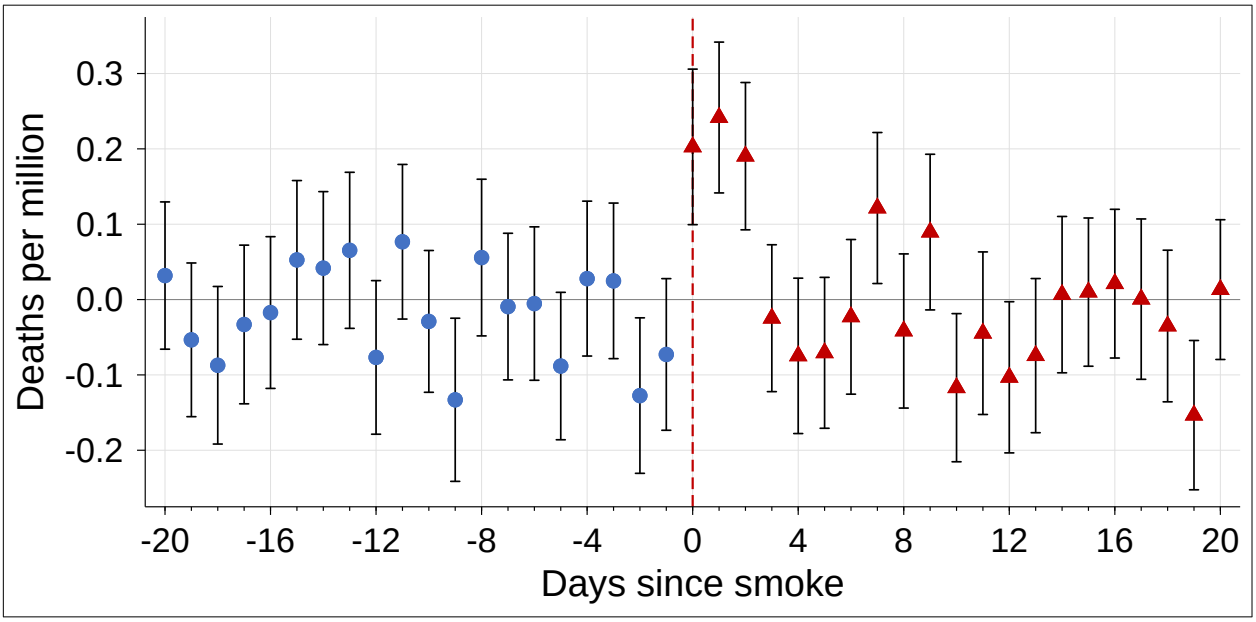


Notes: The figure shows the geographic distribution of days of smoke plume coverage per year across counties during the sample period, 2007–2017. The population-weighted average is 38 days.

Figure 5: Event study of wildfire smoke on pollution and mortality



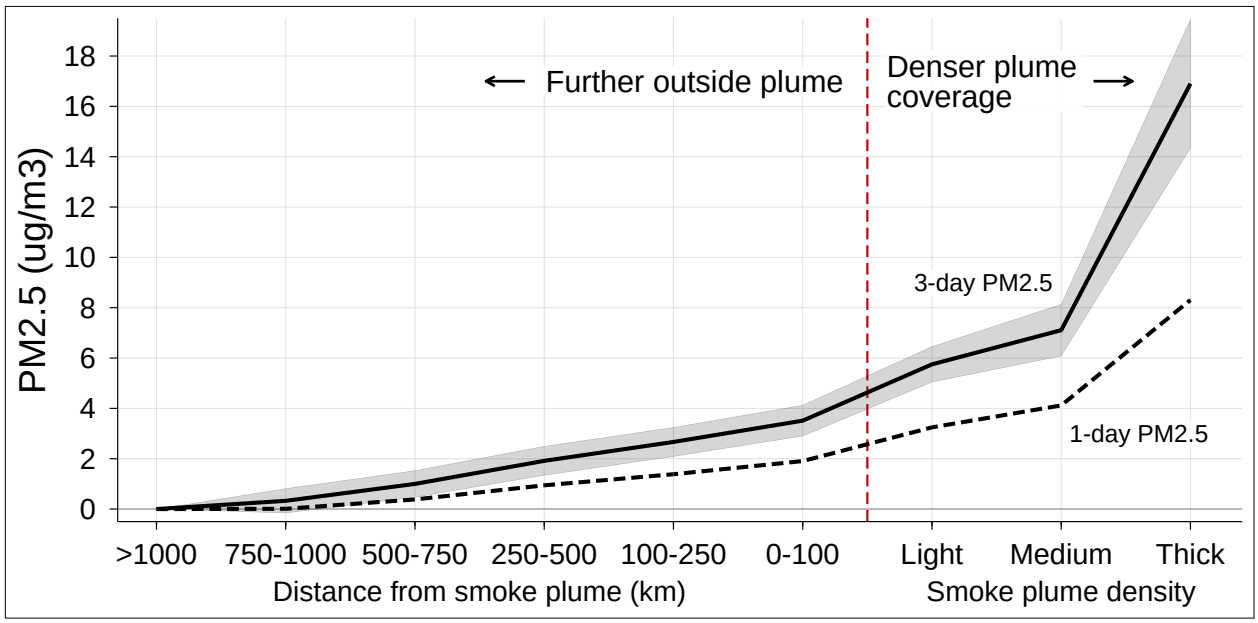
(a) $PM_{2.5}$



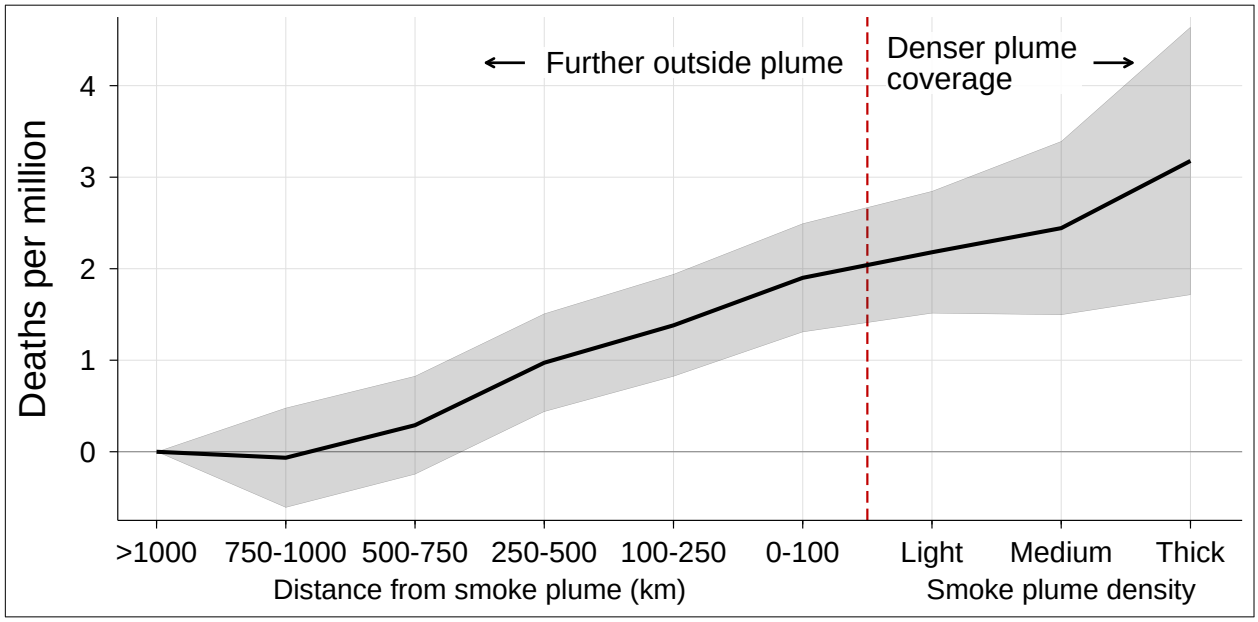
(b) Mortality

Notes: The figure reports event-study estimates from equation (1). Each estimate reflects the effect of a smoke index event in county c on date t on ground-level $PM_{2.5}$ (panel (a)) and deaths per million (panel (b)) on the date of the event (day 0 on the graph) and up to 20 days before (negative day values) and after (positive day values) the event. Regressions are weighted by the Medicare population in county c on date t. Whisker lines reflect 95% confidence intervals based on standard errors are clustered at both the county and date levels.

Figure 6: Effects by intensity of smoke shock



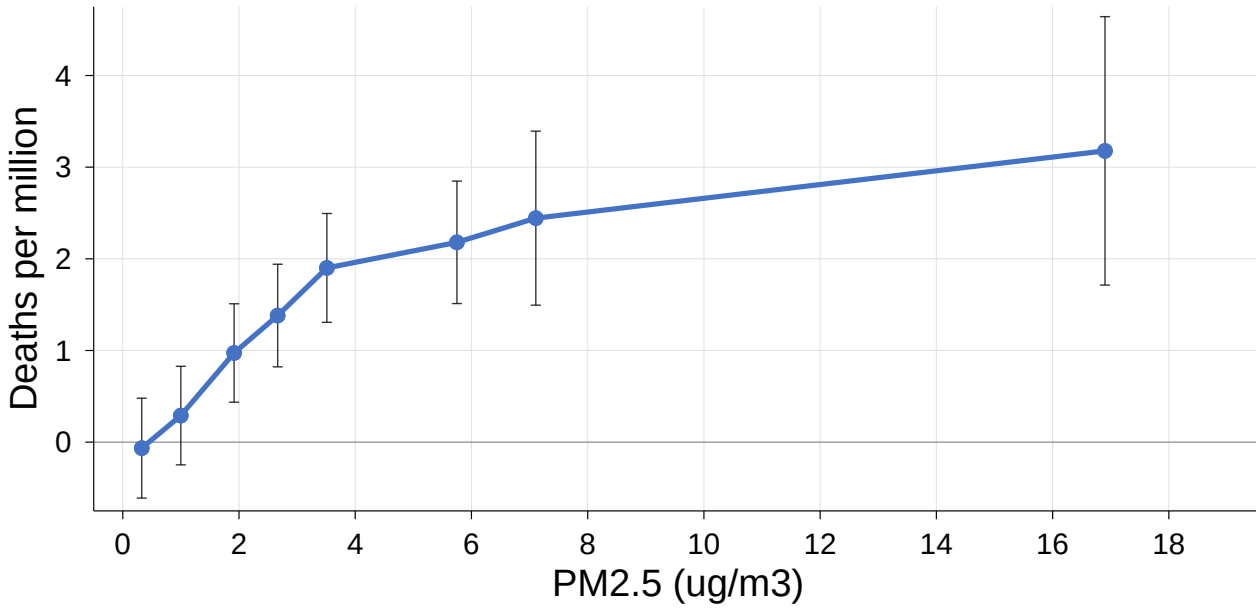
(a) $PM_{2.5}$



(b) Mortality

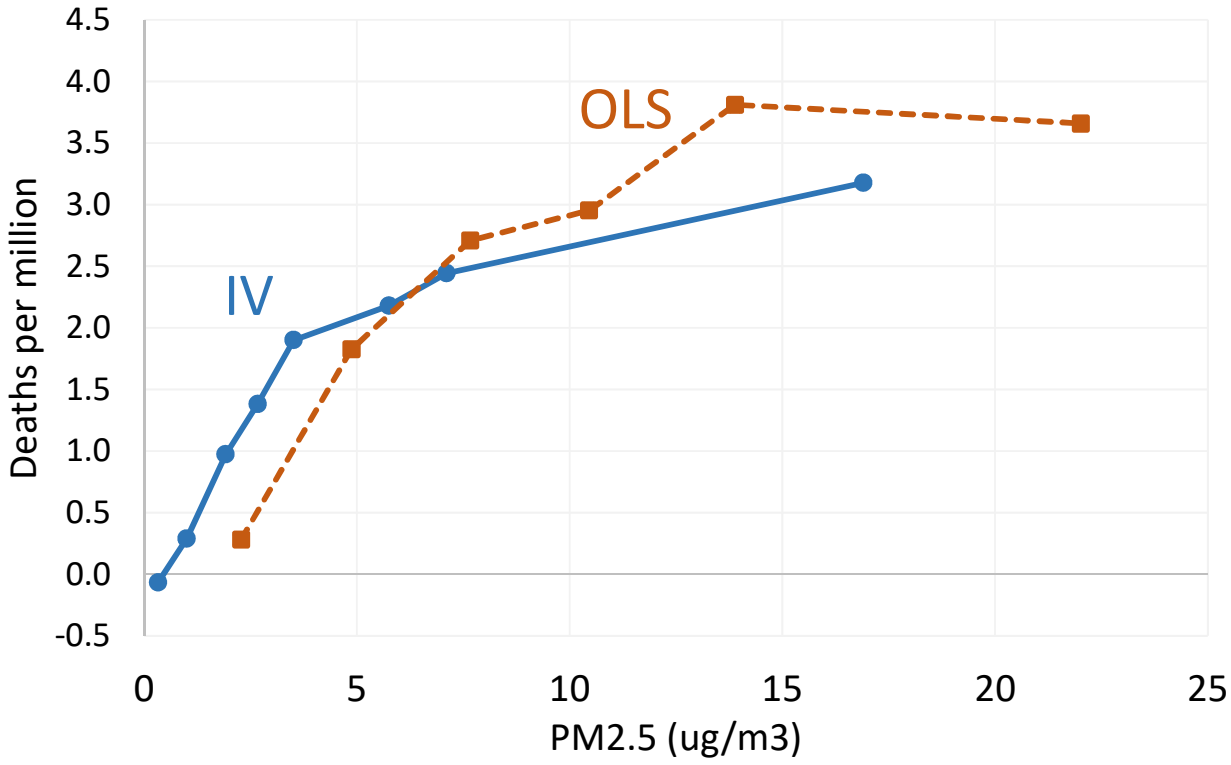
Notes: The figure reports estimated effects of exposure to smoke shocks of varying intensity using equation (2). Panel (a) reports effects on ground-level $PM_{2.5}$ ($\mu g/m^3$), and panel (b) reports effects on 3-day mortality (deaths per million). Each estimate reflects the effect of being exposed to a smoke shock of intensity s, relative to having been at least 1,000 km in distance from a smoke plume. Regressions are weighted by the Medicare population in county c on date t. Shaded areas reflect 95% confidence intervals based on standard errors are clustered at both the county and date levels.

Figure 7: Dose-response function: elderly mortality vs. $PM_{2.5}$



Notes: This figure shows the dose-response relationship between $PM_{2.5}$ and mortality caused by wildfire smoke shocks of varying intensity. Each point on this curve corresponds to one of the 9 smoke shocks included in equation 2. The horizontal position of the point for smoke shock is given by the "dose" effect of the shock (Figure 6a), while the vertical position is given by the mortality effect (Figure 6b).

Figure 8: Instrumental Variables versus Ordinary Least Squares



Notes: IV estimates are those from the dose-response curve shown in Figure 7. OLS estimates come from replacing smoke shocks with bins of $PM_{2.5}$ in the reduced form of IV equation (3).

Tables

Table 1: IV versus OLS estimates of mortality effects of $PM_{2.5}$

IV design:	Large shocks (1)	Small shocks (2)	All shocks (3)	OLS (4)
Dependent variable: 3-day deaths per million				
3-day $PM_{2.5}$	0.18***	0.64***	0.37***	0.16***
	(0.05)	(0.09)	(0.04)	(0.02)
	[0.08, 0.28]	[0.46, 0.82]	[0.28, 0.45]	[0.12, 0.20]
Excl. smoke instruments	Large	Small	All	N/A
Incl. smoke instruments	None	Large	None	N/A
F-statistic	5880.1	2417.2	3726.7	N/A
Dep. var. mean	354.7	354.7	354.7	354.7
Obs.	2,445,503	2,445,503	2,445,503	2,445,503

Notes: The table reports IV estimates of the relationship between 3-day $PM_{2.5}$ ($\mu g/m^3$) and 3-day mortality (deaths per million). Estimates reported in columns (1)–(3) come from equation (3), which includes controls for county-day and state-year-month fixed effects and 2 leads/lags of all smoke shocks. The OLS estimates in column (4) comes from replacing smoke shocks with $PM_{2.5}$ in equation (3). Standard errors are clustered at the county and date levels.

Table 2: Smoke versus wind direction: comparing IV estimates of mortality effects of $PM_{2.5}$

IV design:	Large shocks (1)	Small shocks (2)	All shocks (3)	Wind (4)
Dependent variable: 3-day deaths per million				
1-day $PM_{2.5}$	0.31***	1.06***	0.62***	0.69***
	(0.09)	(0.15)	(0.08)	(0.06)
	[0.13, 0.49]	[0.76, 1.36]	[0.47, 0.78]	[0.57, 0.80]
Excl. smoke instruments	Large	Small	All	N/A
Incl. smoke instruments	None	Large	None	N/A
F-statistic	13783.5	5998.5	8962.5	298
Dep. var. mean	357	3579	357	385
Obs.	3,478,165	3,478,165	3,478,165	1,980,549

Notes: The table reports IV estimates of the relationship between 1-day $PM_{2.5}$ ($\mu g/m^3$) and 3-day mortality (deaths per million). Estimates reported in columns (1)–(3) come from equation (3), which includes controls for county-day and state-year-month fixed effects and 2 leads/lags of all smoke shocks. Wind IV results in column (4) comes from Table 2 of Deryugina et al. (2019).